

1 Altered dorsal CA1 neuronal population coding in the APP/PS1 mouse model of Alzheimer's
2 disease

3

4 Udaysankar Chockanathan^{1,2,3}, Emily Warner^{1,2}, Loel Turpin¹, M. Kerry O'Banion^{1,2,3,5}, Krishnan
5 Padmanabhan^{1,2,4,5}

6 ¹Department of Neuroscience, University of Rochester School of Medicine & Dentistry

7 ²Neuroscience Graduate Program, University of Rochester School of Medicine & Dentistry

8 ³Medical Scientist Training Program, University of Rochester School of Medicine & Dentistry

9 ⁴Center for Visual Science, University of Rochester School of Medicine & Dentistry

10 ⁵Ernest J. Del Monte Institute for Neuroscience, University of Rochester School of Medicine &
11 Dentistry

12

13 correspondence: Krishnan_padmanabhan@urmc.rochester.edu

14 Title: 14

15 Abstract: 73

16 Text: 1375 words

17 Main figure legends: 320

18 Figures: 3

19 Supplemental Methods: 1444 words

20 Supplemental Figures: 16

21

22

23

24

25 **Abstract**

26 While the link between amyloid β ($A\beta$) accumulation and synaptic degradation in
27 Alzheimer's disease (AD) is known, the consequences of this pathology on coding remain
28 unknown. We found that the entropy across neural ensembles was lower in the CA1 region in
29 the APP/PS1 mouse model of $A\beta$, thereby reducing the population's coding capacity. Our
30 results reveal a network level signature of the deficits $A\beta$ accumulation causes to the
31 computations performed by neural circuits.

32

33

34

35

36

37

38

39

40

41

42

43

44

45

46

47

48

49

50

51 **Main Text**

52 Alzheimer's disease (AD) is a progressive neurodegenerative disorder associated with
53 cognitive decline that is thought to arise in part due to the pathological accumulation of amyloid
54 β (A β) plaques¹ throughout the neocortex and hippocampus. Plaques cause a constellation of
55 changes in neural circuits including, but not limited to, degradation of dendritic spines²,
56 reductions in synapse density^{2,3}, and increases in the intrinsic excitability of neurons³. A β
57 pathology has been linked to various behavioral and cognitive changes^{4,5}; for example, plaque
58 burden correlates with degradation of place fields in the dorsal CA1 (dCA1) subfield of the
59 hippocampus resulting in poor performance on spatial memory tasks⁴. Such behaviors require
60 the orchestration of activity across large groups of neurons, or ensembles, whose dynamics are
61 governed by the structure of neural circuits⁶. However, although A β pathology disrupts multiple
62 features of these circuits^{2,7,8}, the net effect of these changes on the structure of population
63 activity and the resulting disruptions in neural computation remain unknown.

64 To address this question, we performed electrophysiological recordings in the
65 hippocampus of awake APP/PS1 mice (model of A β pathology⁹, **Fig. 1a, d**), where dense
66 amyloid plaques can be seen at 12 months of age¹⁰ and correspond to poor performance on
67 spatial cognition and memory tasks, such as the T-maze alternation task^{4,5}. High-density 128
68 channel arrays were targeted to the dCA1 region in head-fixed APP/PS1 and non-transgenic
69 control mice (N = 4 male APP/PS1, N = 4 male control, age = 12-13 months, see **Supplemental**
70 **Methods** for details) trained to run freely on a one-dimensional wheel. Up to 134 well-isolated
71 single units were identified in each animal¹¹ (control = 58 \pm 37 units, APP/PS1 = 59 \pm 50 units, see
72 supplemental methods, **Fig. 1b-c, e-f, S1**). Representative rasters from a control (**Fig. 1g**) and
73 APP/PS1 mouse (**Fig. 1h**) illustrate the complexity of patterns of ensemble activity across both
74 groups.

75 To characterize the statistics of this activity across ensembles in both control and
76 APP/PS1 mice, we first calculated the entropy, a measure of the diversity of patterns of firing
77 that occurred over the duration of the recording^{12,13} (**Fig. 2a, S2**).

78 First, in dCA1, we observed that entropy in APP/PS1 animals was decreased relative to
79 that of controls (control = 0.84 ± 0.45 bits, APP/PS1 = 0.45 ± 0.24 bits, $p < 10^{-6}$, one-sided
80 Wilcoxon rank-sum test, **Fig. 2b**), suggesting that the number of different patterns in APP/PS1
81 animals was smaller than in controls. The reduced entropy in APP/PS1 animals was significant
82 across a range of ensemble sizes varying from 3 to 19 neurons (**Fig. S3, S4**), and was even
83 preserved after normalizing entropy by firing rate (**Fig. S5**).

84 Different behavioral states, such as running or remaining stationary, impact features of
85 both single neuron and population activity¹⁴⁻¹⁶. To understand how these behavioral states
86 affected entropy in control and APP/PS1 mice, the frequency of different patterns of activity was
87 estimated when animals were running and compared to when animals remained stationary (**Fig.**
88 **2c**). First, we found that running increased entropy in both control (stationary = 0.83 ± 0.45 bits,
89 running = 1.04 ± 0.68 bits, $p < 10^{-6}$, one-sided Wilcoxon rank-sum test, **Fig. 2f,h**) and APP/PS1
90 mice (stationary = 0.43 ± 0.24 bits, running = 0.59 ± 0.26 bits, $p < 10^{-6}$, one-sided Wilcoxon rank-
91 sum test, **Fig. 2g,h**). Interestingly, independent of whether the animal was stationary (control =
92 0.83 ± 0.45 bits, APP/PS1 = 0.43 ± 0.24 bits, $p < 10^{-6}$, one-sided Wilcoxon rank-sum test) or
93 running (control = 1.04 ± 0.68 bits, APP/PS1 = 0.59 ± 0.26 bits, $p < 10^{-6}$, one-sided Wilcoxon rank-
94 sum test), entropy was always lower in APP/PS1 animals than controls (**Fig. 2d,e, S6-7**),
95 suggesting that the reduction in the number of possible network patterns was a general feature
96 of ensemble activity. Furthermore, the magnitude of the change in entropy from stationary to
97 running was significantly smaller in APP/PS1 mice than controls. (control = 0.21 ± 0.38 bits,
98 APP/PS1 = 0.16 ± 0.17 bits, $p < 0.005$, one-sided Wilcoxon rank-sum test, **Fig. 2h**). A β pathology
99 thus reduced not only the number of patterns generated by neural ensembles, but also the
100 flexibility of those patterns across behaviors.

101 While the changes in entropy observed in APP/PS1 animals suggested that the diversity
102 of network patterns was reduced with amyloid deposition, it remained unclear why such a
103 reduction occurred. For instance, hypersynchronous neuronal activity, associated with the
104 increased risk of seizures in human AD as well as mouse models^{17,18}, could reduce entropy by
105 increasing the occurrence of patterns of highly correlated neurons. By contrast, a similar, albeit
106 mechanistically distinct reduction in entropy could occur due to the synapse loss and
107 compromised dendritic structure seen in APP/PS1 animals³, which would result in fewer network
108 patterns.

109 To disambiguate these different possibilities, we linked the statistics of network patterns
110 to the functional coupling of neurons using maximum-entropy models that aim to predict
111 patterns of activity with as few *a priori* assumptions of structure as possible^{13,16,19}. For each
112 ensemble, we fit both an independent firing model that only contained a term for the activity of
113 each neuron (\mathbf{h}_i) and a pairwise interaction model that contained the \mathbf{h}_i term for each neuron as
114 well as a term for the functional coupling between pairs of neurons (\mathbf{J}_{ij}) (**Fig. S8**). This allowed
115 us to estimate how cell autonomous properties, such as intrinsic excitability, and cell non-
116 autonomous properties, such as pairwise interactions, shaped the patterns of the network, and,
117 in turn, the entropy. To visualize this, we plotted the predicted patterns from the models and the
118 empirical patterns for a representative control (**Fig. 3a,b**) and APP/PS1 (**Fig. 3c,d**) animal. Each
119 point represents a different pattern and the color denotes the number of active units in that
120 pattern. To quantify the goodness of fits between model and data, we used a measure of the
121 distance between two probability distributions, the Kullbeck-Liebler Divergence (KLD). First, the
122 KLD of the independent firing model was significantly larger for controls than APP/PS1 animals
123 (control = $1.97 \times 10^{-2} \pm 3.39 \times 10^{-2}$, APP/PS1 = $3.81 \times 10^{-3} \pm 6.29 \times 10^{-3}$, $p < 10^{-6}$, one-sided Wilcoxon
124 rank-sum test, **Fig. 3e, S9, S10**), showing that a first order maximum-entropy model better
125 predicted patterns of neuronal activity for APP/PS1 animals than for controls. Additionally, we
126 found that the pairwise interactions model was also better at predicting patterns in APP/PS1

127 animals than controls (control = $9.17 \times 10^{-4} \pm 1.20 \times 10^{-3}$, APP/PS1 = $2.24 \times 10^{-4} \pm 2.88 \times 10^{-4}$, $p < 10^{-6}$,
128 one-sided Wilcoxon rank-sum test, **Fig. 3e, S11**). Interestingly, the J_{ij} terms in APP/PS1 animals
129 were decreased compared to control animals (control = 0.02 ± 1.10 , APP/PS1 = -0.28 ± 1.01 , $p <$
130 0.05 , one-sided Wilcoxon rank-sum test, **Fig. 3g, S12**), suggesting that a model incorporating
131 reductions in functional coupling between neurons, possibly arising from reductions in dendritic
132 length and branching³ or decreased synaptic density², was better able to predict the paucity of
133 dCA1 network patterns (**Fig. S13, S14**).

134 In summary, the decreased entropy observed in APP/PS1 animals revealed a reduction
135 in the diversity of network patterns available to populations of neurons in dCA1. Such a
136 decrease effectively constrains the number of patterns available to represent sensory stimuli or
137 experiences, and this reduction in coding vocabulary could lead to the cognitive and spatial
138 memory impairments seen in APP/PS1 mice⁵ and may provide clues into impairments in human
139 AD^{20,21}.

140 Additionally, we found that maximum-entropy models, both the independent and
141 pairwise models, were better at predicting dCA1 population activity in APP/PS1 animals than
142 controls. While these models do not explicitly reflect circuit level deficits such as synaptic
143 connectivity, they provide insight into how the constellation of cellular and molecular changes in
144 APP/PS1 and related models of AD may result in diminished coding capacity and network
145 function^{2,3}. The counterintuitive result that the pairwise interactions model was better able to
146 account for dCA1 activity in APP/PS1 animals than controls suggests that once a change in
147 functional coupling was accounted for, there was sufficient information to describe the diversity
148 of network patterns in APP/PS1 animals. By contrast, in controls, the inclusion of pairwise
149 interactions was still insufficient to predict the observed network patterns. The structure of
150 activity patterns in control animals is therefore likely shaped by higher order interactions²²
151 (triplet, quadruplet, etc.) that are either diminished or absent in APP/PS1 animals. Previous
152 studies have identified the role that these higher-order interactions play in shaping population

153 activity in sensory systems and implicated the local circuits that give rise to such higher-order

154 interactions¹³; our results hint at their importance in dCA1 and the extent to which they may be

155 especially vulnerable to A β pathology in APP/PS1 animals.

156

157 **References**

- 158 1. Braak, H., Thal, D.R., Ghebremedhin, E. & Tredici, K. *Del J. Neuropathol. Exp. Neurol.*
159 **70**, 960–969 (2011).
- 160 2. Tsai, J., Grutzendler, J., Duff, K. & Gan, W.-B. *Nat. Neurosci.* **7**, 1181 (2004).
- 161 3. Šišková, Z. et al. *Neuron* **84**, 1023–1033 (2014).
- 162 4. Cacucci, F., Yi, M., Wills, T.J., Chapman, P. & O’Keefe, J. *Proc. Natl. Acad. Sci.* **105**,
163 7863–7868 (2008).
- 164 5. Webster, S.J., Bachstetter, A.D. & Van Eldik, L.J. *Alzheimers. Res. Ther.* **5**, 28 (2013).
- 165 6. Yuste, R. *Nat. Rev. Neurosci.* **16**, 487 (2015).
- 166 7. Busche, M.A. et al. *Science* **321**, 1686–1690 (2008).
- 167 8. Walsh, D.M. et al. *Nature* **416**, 535 (2002).
- 168 9. Jankowsky, J.L. et al. *Biomol. Eng.* **17**, 157–165 (2001).
- 169 10. Liebmann, T. et al. *Cell Rep.* **16**, 1138–1152 (2016).
- 170 11. Lewicki, M. *Netw. Comput. Neural Syst.* **9**, R53–R78 (1998).
- 171 12. Schneidman, E., Bialek, W. & Berry II, M.J. *J. Neurosci.* **23**, 11539–11553 (2003).
- 172 13. Ohiorhenuan, I.E. et al. *Nature* **466**, 617–621 (2010).
- 173 14. Niell, C.M. & Stryker, M.P. *Neuron* **65**, 472–479 (2010).
- 174 15. Vinck, M., Batista-Brito, R., Knoblich, U. & Cardin, J.A. *Neuron* **86**, 740–754 (2015).
- 175 16. Meshulam, L., Gauthier, J.L., Brody, C.D., Tank, D.W. & Bialek, W. *Neuron* **96**, 1178-
176 1191.e4 (2017).
- 177 17. Minkeviciene, R. et al. *J. Neurosci.* **29**, 3453–3462 (2009).
- 178 18. Vossel, K.A. et al. *JAMA Neurol.* **70**, 1158–1166 (2013).
- 179 19. Schneidman, E., Berry, M.J., Segev, R. & Bialek, W. *Nature* **440**, 1007–1012 (2006).
- 180 20. Cao, D., Lu, H., Lewis, T.L. & Li, L. *J. Biol. Chem.* **282**, 36275–36282 (2007).
- 181 21. Fitten, L.J. et al. *JAMA* **273**, 1360–1365 (1995).
- 182 22. Ganmor, E., Segev, R. & Schneidman, E. *Proc. Natl. Acad. Sci.* **108**, 9679–9684 (2011).

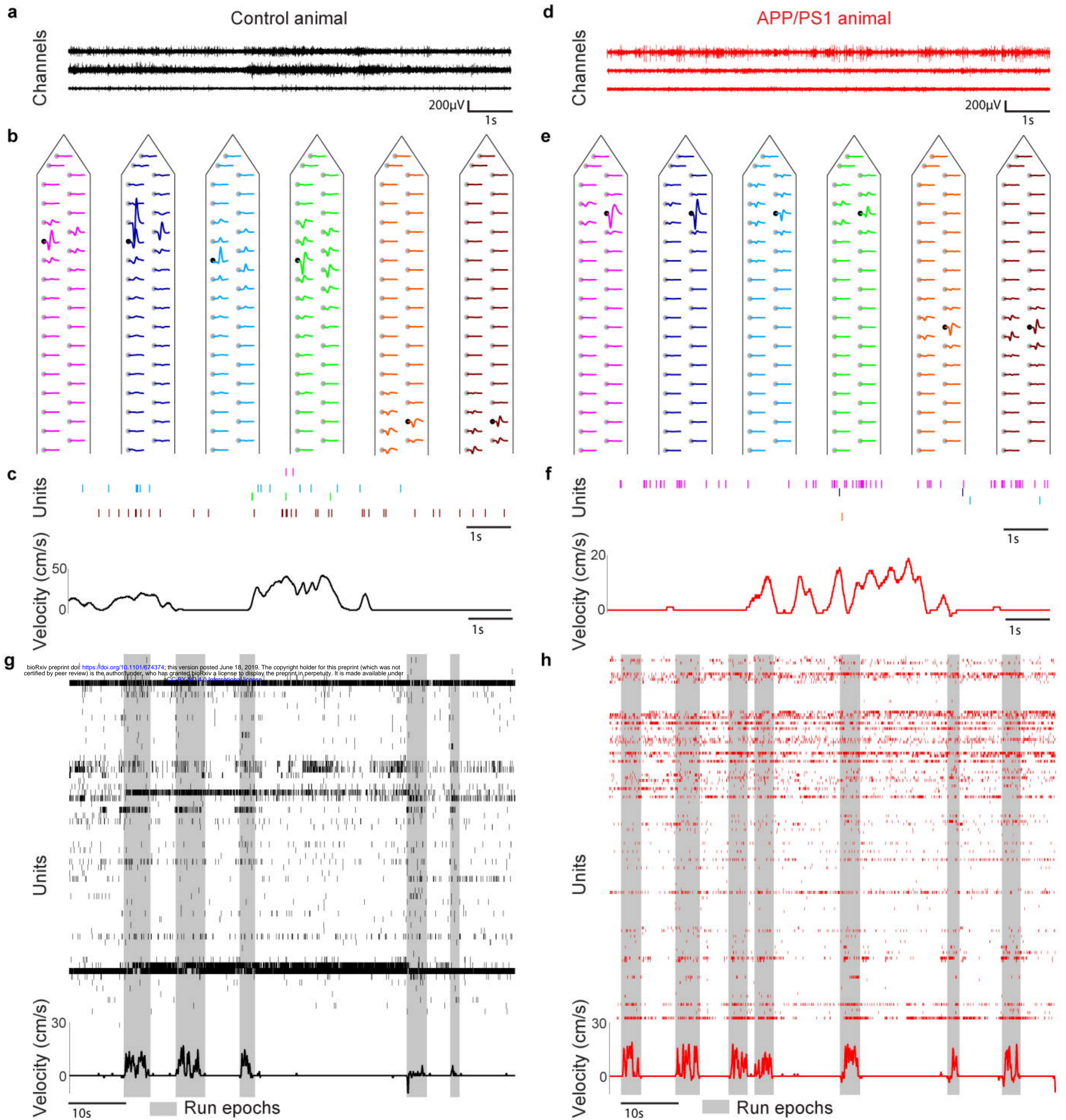


Figure 1 High-density awake recordings of dCA1 neuronal populations. (a,d) 10-second interval of raw electrophysiology data from three channels. (b,e) Mean waveform of each unit from channels in a and d as it appeared on the channel on which it was detected (black circle) and on the other channels on the electrode shank (grey circles). (c,f) Raster plot of sorted units and running velocity. Each tick denotes an action potential. (g,h) Raster plot of all units isolated in a representative control (g) and APP/PS1 (h) animal and simultaneous running behavior.

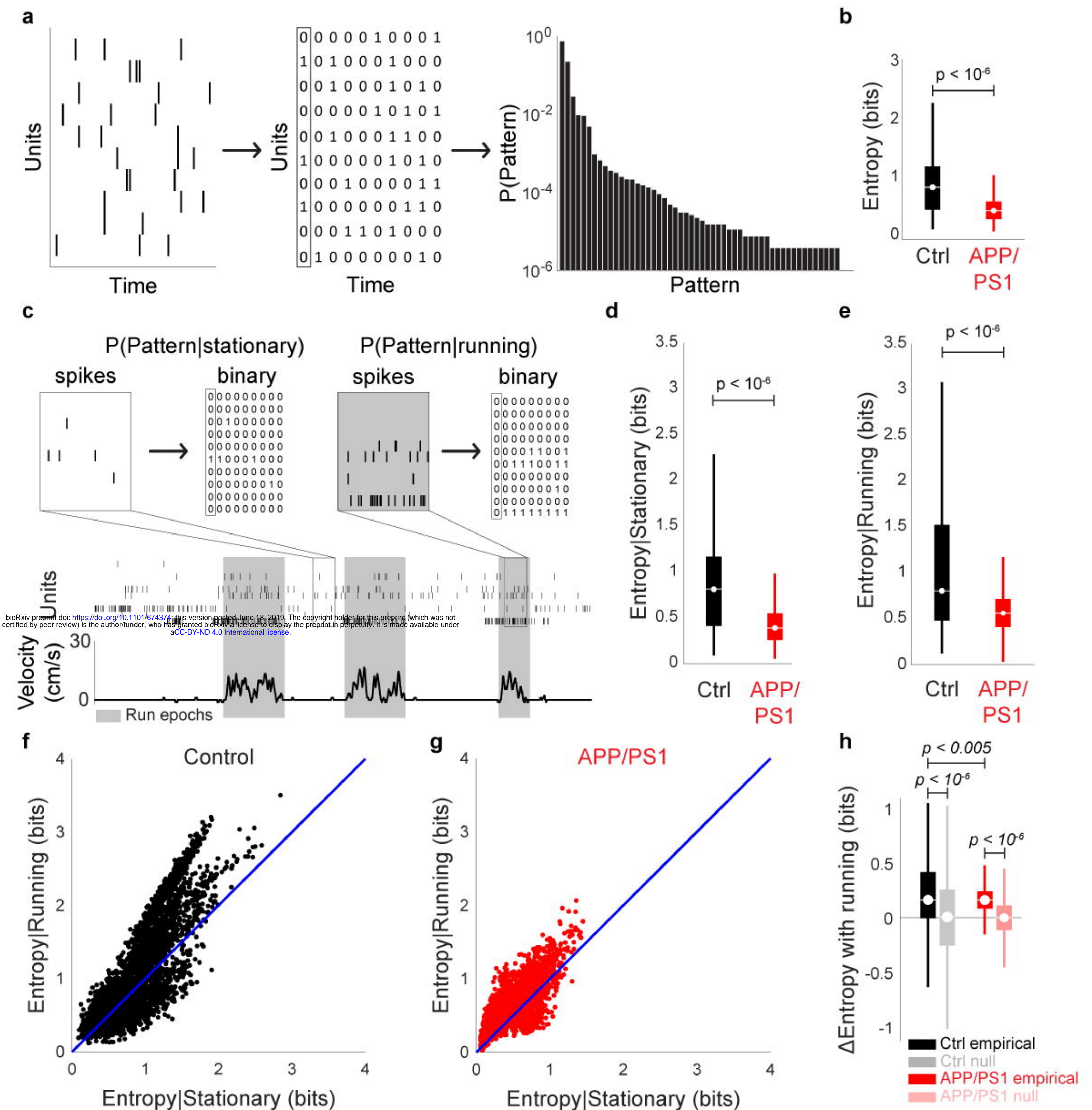


Figure 2 Entropy of dCA1 neuronal populations (a) Schematic of entropy calculation. (b) The APP/PS1 group had significantly lower entropy than controls. (c) Schematic of entropy calculation conditioned on behavioral state. (d,e) For both stationary (d) and running (e) conditions, the entropy of APP/PS1 animals was lower than that of controls. (f,g) Comparison of entropy for stationary and running entropy. (h) Entropy change with running. Null distributions were generated from a Gaussian centered at 0 with the same standard deviation as the corresponding empirical distributions. Both control and APP/PS1 animals exhibited a significant increase in entropy with running. However, the magnitude of this increase was larger in controls than APP/PS1 animals.

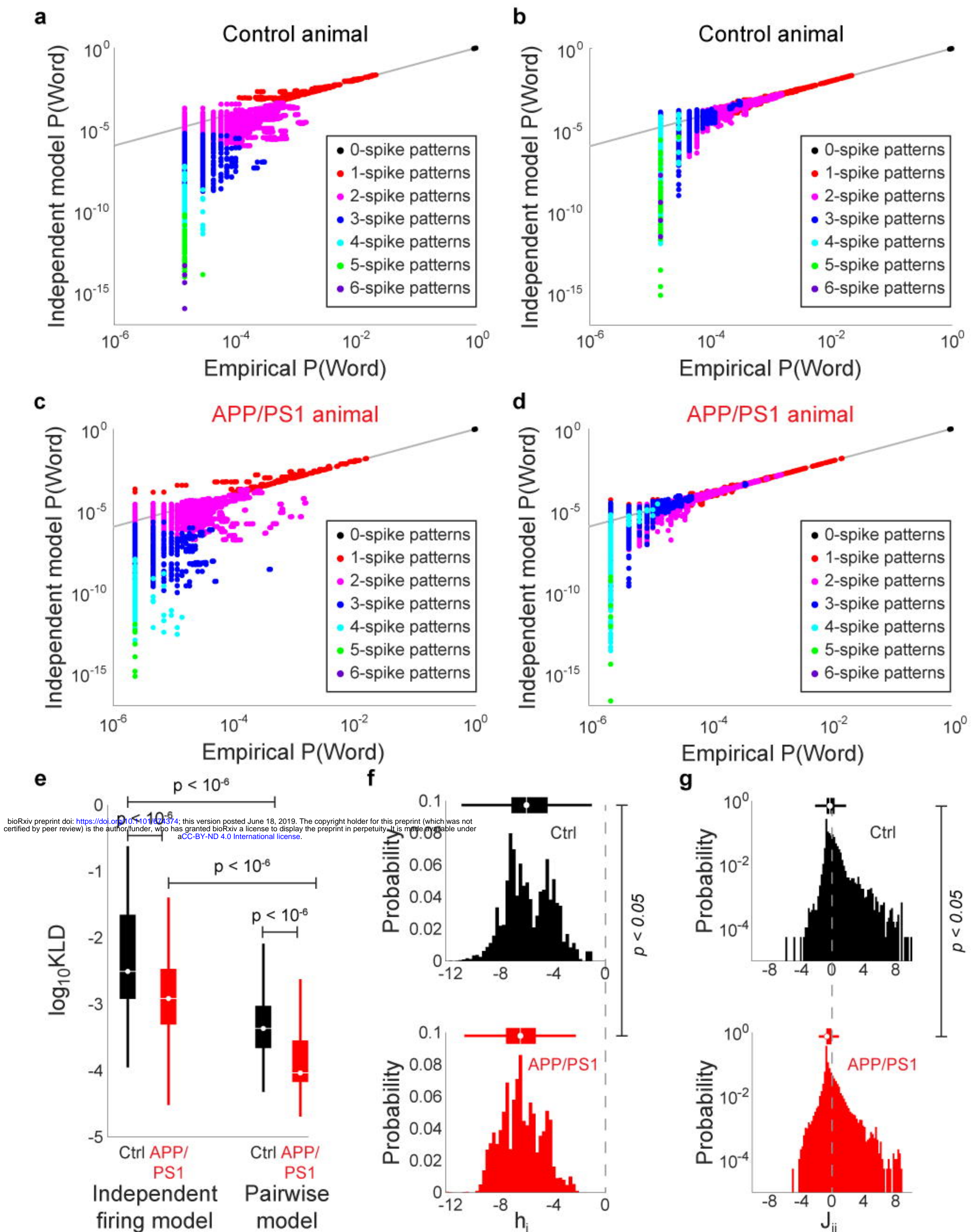


Figure 3 Maximum entropy models of dCA1 neuronal populations in control and APP/PS1 mice (**a-d**) Comparison of predicted and model word probabilities for a representative control (**a,b**) and APP/PS1 (**c,d**) animal for the independent model (**a,c**) and pairwise model (**b,d**). Colors denote the number of coactive neurons in each word. (**e**) Kullback-Liebler divergence (KLD) between empirical and model word probability distributions. For both models, the KLD was smaller for APP/PS1 mice than controls. Moreover, the pairwise models for both control and APP/PS1 groups had a lower KLD than the corresponding independent models. (**f,g**) Histograms of (**f**) h_i and (**g**) J_{ij} terms. Dashed line denotes 0. Both h_i and J_{ij} terms were smaller in the APP/PS1 group than the controls.